The Egyptian Journal of Remote Sensing and Space Sciences (2015) 18, 297–310

HOSTED BY

National Authority for Remote Sensing and Space Sciences

The Egyptian Journal of Remote Sensing and Space Sciences

www.elsevier.com/locate/ejrs
www.sciencedirect.com

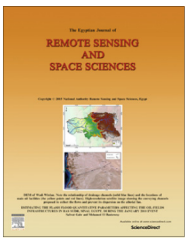

RESEARCH PAPER

Soil moisture retrieval model by using RISAT-1, C-band data in tropical dry and sub-humid zone of Bankura district of India

Kousik Das [a,*], **Prabir Kumar Paul** [b]

[a] *Geoinformatics, Department of Mining Engineering, Indian Institute of Engineering Science and Technology, Shibpur, 711103 Howrah, W.B., India*
[b] *Department of Mining Engineering, Indian Institute of Engineering Science and Technology, Shibpur, 711103 Howrah, W.B., India*

Received 28 June 2015; accepted 17 September 2015
Available online 20 October 2015

KEYWORDS

SAR;
RISAT-1;
Soil moisture;
Semi-empirical model

Abstract Soils play a key role in various hydrological and meteorological applications. The objective of this paper is to analyze the spatial variability of very high resolution (3.3 m) RISAT-1 (5.35 GHz) data with surface soil parameters to produce soil moisture retrieval model. The behaviors of the RISAT-1 signal were analyzed for two configurations, RH and RV at high incident angle (48.11°), with regard to several soil conditions: volumetric moisture content (M_v), root mean square surface roughness (*r.m.s.*) and soil composition (texture). The relationship between the backscattering coefficient ($\sigma°$) and the soil parameters (moisture, surface roughness and texture) was examined by means of satellite images, as well as ground truth measurements, of each of the 23 plots, recorded during several field campaigns in the January 2015. RISAT-1 images demonstrate high potential for the identification of local variations of soil dielectric constant (ε), texture and M_v. $\sigma°$ has a positive relationship with M_v both for $\sigma°$ (RH) and $\sigma°$ (RV) with $R^2 = 0.588$ and $R^2 = 0.525$. The roughness component was derived in terms of *r.m.s.* having a positive correlation with $\sigma°$ (RH) ($R^2 = 0.009$) and $\sigma°$ (RV) ($R^2 = 0.029$). Dielectric constant (ε) has a positive relationship with $\sigma°$ (RH) having $R^2 = 0.656$ and $\sigma°$ (RV) having $R^2 = 0.534$. By considering all the major influencing factors ($\sigma°$ (RH), $\sigma°$ (RV), ε and *r.m.s.*) a semi-empirical model has been developed, where M_v is a function of $\sigma°$ (RH), $\sigma°$ (RV), ε and *r.m.s.* This model has adjusted $R^2 = 0.956$ and RMSE = 0.010 at 95% confidence level.

1. Introduction

In hydrologic studies, soil moisture is a critical component as it controls the partitioning between infiltration and runoff. Infiltration determines the amount of water available for vegetation growth and runoff has a strong impact on the rate of

* Corresponding author. Mobile: +91 9748418579.
E-mail address: kousik.envs@gmail.com (K. Das).
Peer review under responsibility of National Authority for Remote Sensing and Space Sciences.

http://dx.doi.org/10.1016/j.ejrs.2015.09.004

surface erosion and river processes (Álvarez-Mozos et al., 2005; Wagner et al., 2007; Zhao and Li, 2013; Al-Yaari et al., 2014). The wetness of the soil also controls the evapotranspiration rate and thus the micro-meteorology. Especially information on the spatial distribution of soil moisture, caused by micro-topography, vegetation, and stochastic precipitation events, is of major importance for watershed management, as it allows for optimizing the reallocation of water supplies during dry periods, or aids in predicting and managing high tides and floods during extreme rainfall events. In each of these cases knowledge of the distribution and amount of water in the soil can aid developing better modeling and decision support tools (Seneviratne et al., 2010; Kornelsen and Coulibaly, 2013; Petropoulos et al., 2015).

Technological advances in satellite remote sensing have offered a variety of techniques for measuring soil moisture across a wide area continuously over time (Engman, 1990). Thus direct observations of soil moisture are currently restricted to discrete measurements at specific locations, because soil moisture is highly variable both spatially and temporally (Engman, 1991; Wood et al., 1992; Laguardia and Niemeyer, 2008) and are therefore inadequate to carry out regional and global studies (http://www.geotimes.org/may02/WebExtra0503.html). Soil-moisture information can be retrieved from different remote sensing methods using different data, such as visible, infrared, thermal, and microwave data (Batlivala and Ulaby, 1977; Seneviratne et al., 2010; Petropoulos et al., 2015). Each remote sensing method used has its own advantages and disadvantages, based on how sensitive the soil surface is to the electromagnetic radiation and how strong the reflected radiation, from the soil surface, can be received by the sensor (Batlivala and Ulaby, 1977; Giacomelli et al., 1995; Seneviratne et al., 2010; Petropoulos et al., 2015).

Knowledge of soil surface conditions, soil moisture content, and roughness is of the highest importance in agriculture and vegetation growth monitoring, atmospheric sciences, and hydrological studies (Anguela et al., 2010; Kornelsen and Coulibaly, 2013; Bertoldi et al., 2014). In this context, satellite imagery is a powerful tool that can provide accurate and repetitive spatial data. Synthetic-aperture radar (SAR) techniques are particularly useful because they make it possible to monitor soil parameters under any weather conditions (Dobson and Ulaby, 1986; Fung, 1994; Hallikainen et al., 1985; Ulaby et al., 1986; Kornelsen and Coulibaly, 2013). For bare agricultural soils, the backscattered radar signal depends strongly on the geometric characteristics (roughness) and dielectric properties (moisture content, soil composition) of the soil (Singh and Kathpalia, 2007; Li et al., 2014; Gharechelou et al., 2015). Studies of Zribi and Dechambre (2002a,b) using simulation models or experimental analysis have shown that the radar signal is more sensitive to surface roughness at high incidence angles than at low incidence angles (Fung, 1994; Baghdadi et al., 2002a,b, 2008, 2012). Many studies using data collected by space and airborne SAR scatterometers and model simulations have already shown the potential of radar data to retrieve soil parameters (roughness and moisture) and, to a lesser extent, to the soil's textural composition (Baghdadi et al., 2002a,b, 2006; Baghdadi et al., 2007; Dobson and Ulaby, 1986; Fung and Chen, 1992; Holah et al., 2005; Le Hégarat Mascle et al., 2002; Oh, 2004; Shi et al., 1997; Srivastava et al., 2003, 2006, 2009; Ulaby et al., 1978; Zribi et al., 2005). Whatever the SAR configuration, the radar signal follows a logarithmic function with the soil-surface roughness (Fung, 1994; Ulaby et al., 1986). Ulaby et al. (1978) have. The dynamics of the relationship between the radar signal and roughness parameter are stronger in the L-band than in the C- and X-bands (Baghdadi et al., 2008; Ulaby et al., 1986) Moreover, SAR data are more sensitive to soil roughness at high incidence angles (Baghdadi et al., 2008; Baghdadi and Zribi, 2006; Zribi and Dechambre, 2002a,b).

The surface area of soil particles in a soil depends on the particle sizes which control the percentage of free and bound water (Srivastava et al., 2009). Few studies have analyzed the response of the radar signal to soil composition in terms of grain-size distribution based on percentages of sand and clay. The grain-size distribution has an effect on dielectric behavior over the entire frequency range (1.4 to 18 GHz) and is most pronounced at frequencies below 5 GHz (Hallikainen et al., 1985). In the C-band, decreasing soil clay content increases the sensitivity of the radar signal to soil moisture (0.22 dB/% for clay soil: 49% clay, 35% silt and 16% sand; 0.33 dB/% for loamy soil: 17% clay, 48% silt and 35% sand) (Ulaby et al., 1978). As the distribution of grain sizes controls the amount of free water that interacts with the incident microwave, the amount of free water gives significant contribution to SAR backscatter (Srivastava et al., 2006, 2009).

Bankura district is situated between 22°38′ and 23°38′ north latitude and between 86°36′ and 87°46′ east longitude. Climatic condition (e.g., rainfall, temperature and humidity), various complex land form, hydrology and soil combination have greatly influenced the farming system of Bankura district. In Bankura district two Agro Climatic Zones, *viz.,* Undulating Red and lataritic in Sonamukhi, Joypur, Bishnupur, Ranibandh, Gangajalghati, Borjora, Saltora, Onda, Taldangra, Simlapal, Mejhia, Raipur, Sarenga, Chhatna, Indpur, Khatra, Hirbandh, Bankura-I and Bankura-II blocks and Vindhyan Alluvial Zone in Patrasayer, Indus, Kotulpur blocks, exists. Agriculture in this region is mostly rain dependent. Ground water is not easily and economically trappable over there. Prevalence of moisture stress on standing Kharif Crop in late monsoon period is very common. Soil moisture has a great importance for agriculture in the place where water table goes down in late monsoon. Thus the study has been initiated in part of Onda, Taldangra, Simlapal and Bishnupr blocks of Bankura district to retrieve soil moisture by using remote sensing technology. Continuous monitoring of soil moisture is possible throughout the year by using remote sensing technology on this sub-humid and dry region. Thus the aim of this work is to derive a model to retrieve volumetric soil moisture content (M_v) by using SAR data. This model can be developed by considering the major influencing factors to retrieve soil moisture in terms of soil physical characteristics (Surface roughness, dielectric constant and soil texture) and sensor configuration (back scattering coefficient including both polarizations, (RH and RV)).

2. Materials and methods

2.1. Study site

Bankura district is situated between 22°38′ and 23°38′ north latitude and between 86°36′ and 87°46′ east longitude

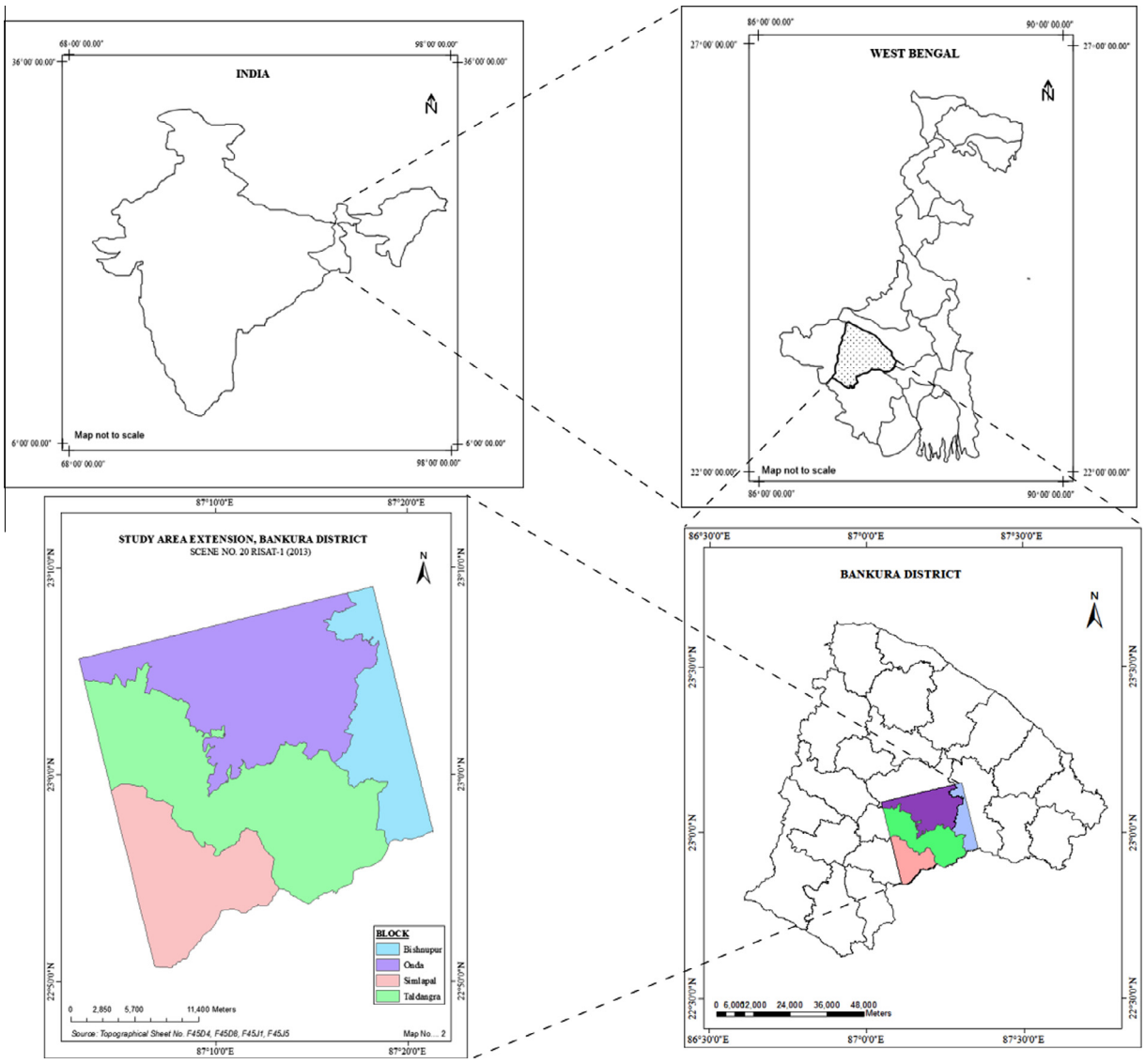

Figure 1 Representation and location map of study area.

(Fig. 1). With a triangle shaped contour, the district lies in the Burdwan Division of West Bengal. The Damodar river separates Bankura from Burdwan district in the north. The district of Midnapore and Purulia share its southern and western boundaries respectively with Bankura. The south-eastern part of the district is bounded to a certain extent by Hooghly district. The part of Bankura district which has been taken into consideration for study is lying within 22°51′54.23″ N, 87°22′42.83″E to 23°5'33.58″N 87°22'42.83″E (Fig. 2). Parts of Bishnupr, Simlapal, Onda and Taldangra block of Bankura district are lying within this geographical extension, which have been studied (Fig. 2). The soil, however, in the other blocks consists of sandy loam and Clay loam. The study area is tropical dry and sub-humid having yearly rainfall of 1480.62 mm in last five years from 2009 to 2013 mm and maximum temperature ranges between 45 °C maximum and minimum of 10 °C normally. Rainfall data have been collected from INDIA METEOROLOGICAL DEPARTMENT (http://www.imd.gov.in/section/hydro/distrainfall/webrain/wb/bankura.txt).

2.2. Satellite data

2.2.1. SAR data

Radar Satellite-1 (RISAT-1) is a state of the art Microwave Remote Sensing Satellite carrying a Synthetic Aperture Radar (SAR) Payload operating in C-band (5.35 GHz). RISAT-1 was successfully launched by PSLV-C19 on April 26, 2012. It started beaming images from 01 May 2012. The choice of C-band frequency of operation and RISAT-1 SAR capability of imaging in HH,VV,HV,VH and circular polarizations has ensured its wide applicability. As it is a side looking active sensor, around 107 km on either side of the sub-satellite track comes under Non Imageable area for the orbit under consideration.

RISAT-1 (SAR) image was purchased from NRSC Data Centre. The collected image is covering the concerned study area portion of Bishnupr, Simlapal, Onda and Taldangra block of Bankura district under Scene 20, Session 1. The purchased image is Level 2, Fine resolution STRIPMAP (FRS-1)

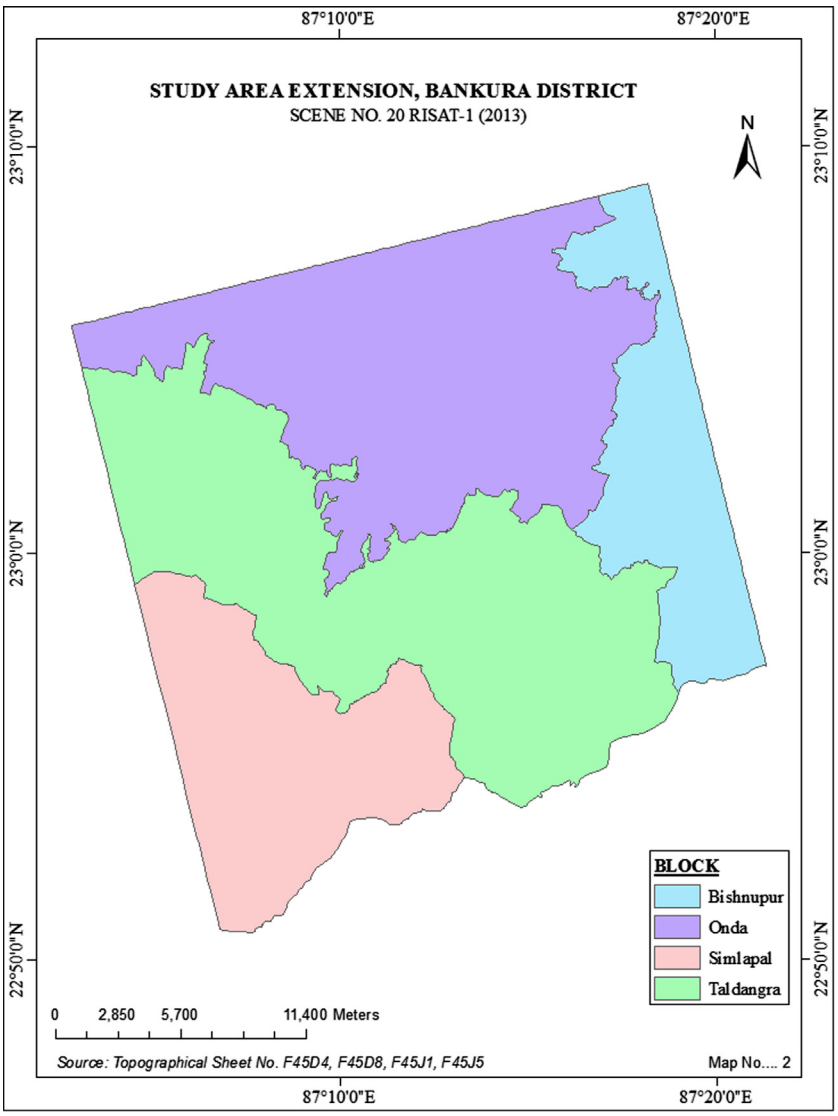

Figure 2 Study area extension; Part of Simlapal, Taldangra, Onda nad Bishnupur block of Bankura district.

mode Terrain Geo-referenced product. The projection system used for this image is WGS_1984_UTM_Zone_45N and Datum: WGS_84. This image is acquired in Right circular polarized mode (RH and RV). The acquisition date of scene is 4th January, 2013, with an orbit No. 3824, look direction right and incidence angle of 48.106 with 3.3 m ground resolution.

2.2.2. Optical data

Land use/land cover map has been prepared by digitizing the image of WorldView-2 satellite sensor, having ground resolution 0.5 m and image acquisition date January/2010. The projection system used for this image is WGS_1984_UTM_Zone_45N and Datum: WGS_84. NDVI map was prepared by using the Landst-7 image acquired in January, 2013. The Landst-7 images of corresponding study area were downloaded from USGS Earth Explorar (https://earthexplorer.usgs.gov).

2.3. Experimental measurements

The field campaigns presented in this study were carried out on the 2nd to 6th of January, 2015. A total of 23 field sites were selected for sampling (Fig. 3). Soil samples per site were collected in 0–5 cm depth of soil surface. GCP (Ground Control Point) for each of the 23 locations were collected at the same time. GCP were collected by using Xploris 400 a handle GPS. During the time of field data collection the humidity of that area was very low. Actual rainfall of Bankura district from 1.03.2015 to 18.03.2015 was 2.2 mm (http://www.imd.gov.in/section/hydro/dynamic/rfmaps/districtwise.htm).

2.3.1. Surface roughness

Measurements of soil roughness were carried out in all of the 23 training plots using roller chain by following standard method (Saleh, 1993). Random roughness profiles across the direction of tillage (five perpendiculars) were established in

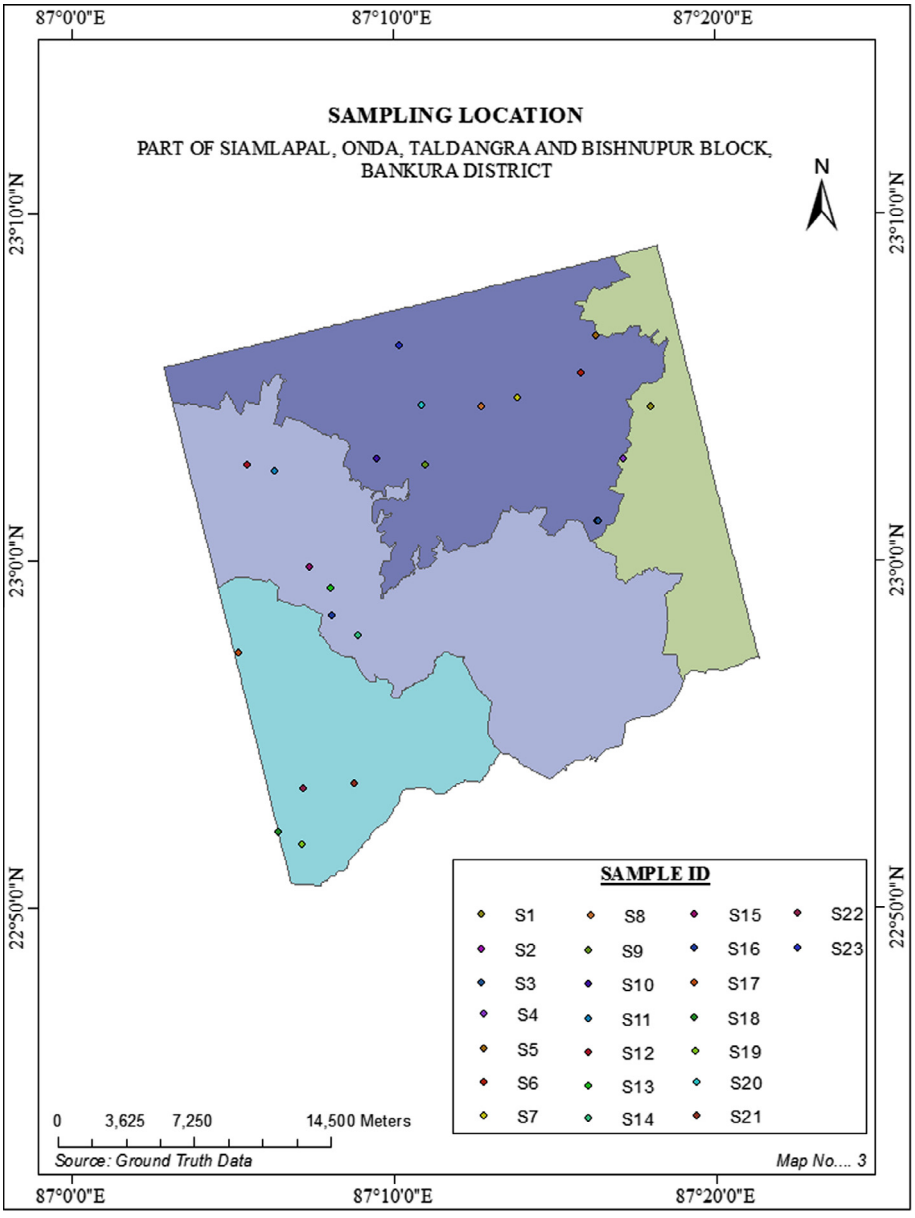

Figure 3 Representation of sampling locations.

each training plot. Soil surface roughness was measured by the chain method by using 0.01 m (0.03 ft) linked roller (ANSI 35 riv.type) chain with a length of 1 m (3.2 ft) ($L1$–1 m) which was very carefully laid out on the soil surface in perpendicular direction to the ridges. A Stanley measuring tape was used to read the linear distance, $L2$, resulting from roughness elements. After obtaining readings from all sites, the average value was used to calculate the random roughness using Eq. (1).

$$C_r = \left(1 - \frac{L_2}{L_1}\right) \times 10 \tag{1}$$

where: C_r, is roughness at any direction. However, roughness caused by aggregates (random roughness) is obtained by measuring the C in perpendicular direction to ridges. $L1$ is the length of roller chain and $L2$ linear distance of chain due to roughness. The statistical properties of the roughness can be explained by the root mean square height ($r.m.s.$) (vertical variation). Root mean square height was calculated using the Eq. (2).

$$r.m.s. = \sqrt{\frac{\sum_{i=0}^{n}(Z_i - \bar{Z})^2}{n-1}} \tag{2}$$

where: Z_i denotes the height of the point, $\bar{Z}$ is the mean height and n is the total number of points taken under consideration.

2.3.2. Soil moisture content

Gravimetric soil moisture (mg) value was obtained from laboratory analysis, which was converted to volumetric soil moisture (M_v) by multiplying bulk density (Sbd) (Eq. (3)):

$$M_v = \text{mg} \times Sbd \tag{3}$$

2.3.3. Soil composition

Soil is the major factor of the vegetation and agriculture as well as runoff assessment. Textural Soil of the study area has been grouped into five types of soils on the basis of analysis of collected samples from 23 sampling sites. These are (i) loamy, (ii) sandy loam, (iii) sandy clay loam, (iv) clay and (v) clay loam. The most abandoned type of soil texture is clay loam (39.13%), sandy clay loam (26.09%) and subsequently loamy type (17.39%). Clay (8.7%) and sandy loam (8.7%) are found in a very smaller portion of the studied sampling sites.

3. Results

3.1. Rainfall

The rainfall data collected were used to find out the average rainfall for the month of January. Along with the average rainfall it was also investigated whether the study area has been affected by rainfall or not prior the days of sampling, during satellite overpasses and the time of field measurements. Five years average rainfall in the month of January of Bankura district is 11.9 mm. Rainfall from October 2012 to January 2013 goes to lowest from 38.0 to 0.9 mm. From this observation it could be concluded that the study area is not affected by the rainfall prior to the days of satellite overpasses. So rainfall does affect normal soil moisture condition of the study area during or before the satellite overpasses. Also it was confirmed that rainfall did not affect the normal soil moisture condition during the field sampling of 2nd to 6th of January, 2015. It was reported that actual mean rainfall of Bankura district from 1.03.2015 to 18.03.2015 is 2.2 mm. It showed that normal soil moisture content was also not affected during or prior to the field sampling of 2nd to 6th of January, 2015.

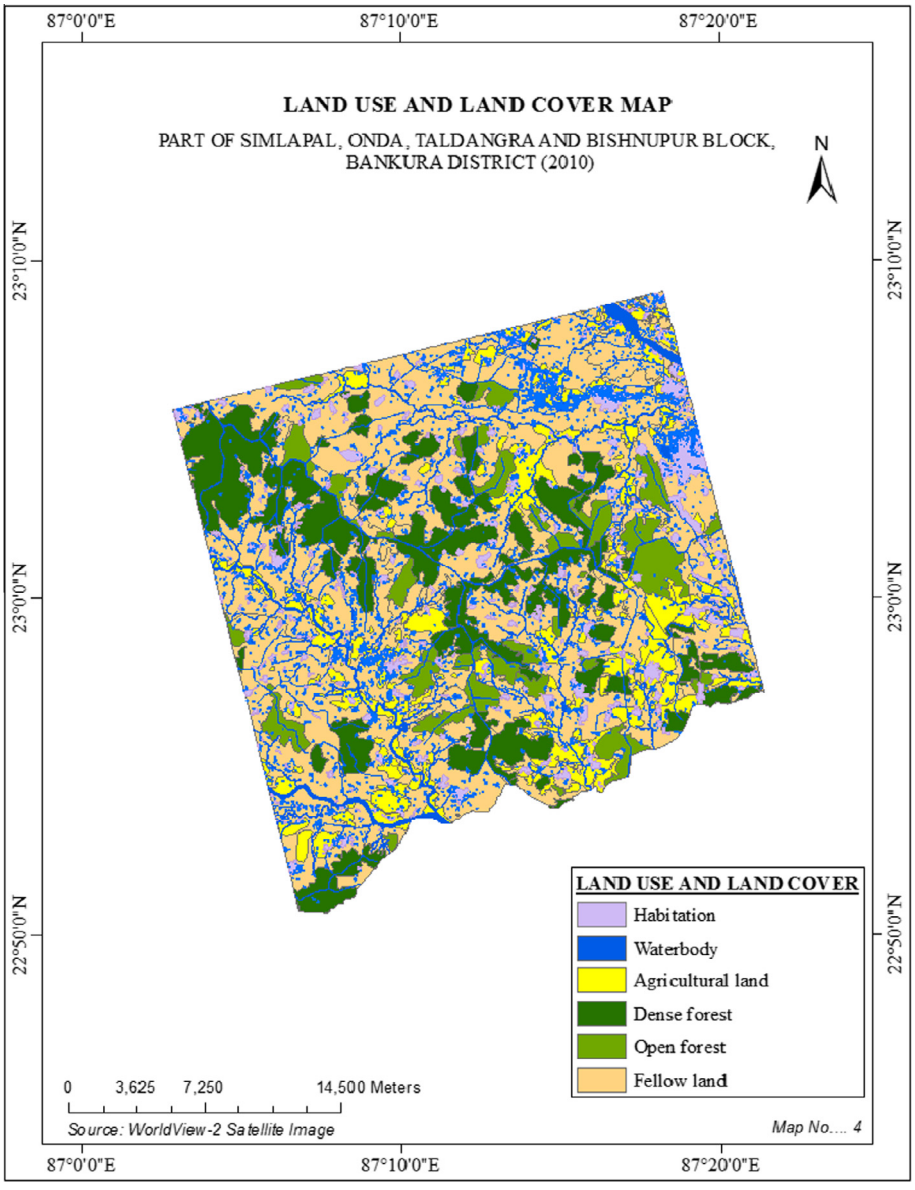

Figure 4 Land use and land cover map of Bankura district, covering part of Simlapal, Taldangra, Onda and Bishnupur block.

3.2. Land use and land cover

Land use and land cover map of the study area was prepared using the WorldView-2 image by digitizing the objects. Simple first level of classification was used for the land use and land cover map. Due care was taken in digitizing the object for desired classes. Basic visual and digital interpretation parameters were followed such as; tone, texture, shape, size, pattern, location and association for the recognition of objects and their tonal boundaries. The final classified output image was assigned 6 classes (Classes are habitation, water body, agricultural land, dense forest, open forest and fallow land) (Fig. 4). 12.66% of total area was found to be under cultivated land which was recognized as agricultural land, 2.84% area is covered by water body, 19.52% under dense forest, 8.25% area under open forest, 0.001% area under habitation and 56.73% area to be occupied fallow land (Table 1). Total area (Km^2) covered by each of the classes is represented in Table 1.

Table 1 Landuse area statistics.

Land use and land cover class	Area (Sq km)	Area (%)
Agricultural field	86.24	12.66
Dense forest	132.99	19.52
Open forest	56.18	8.25
Water body	19.37	2.84
Habitation	0.01	0.00
Fallow land	386.42	56.73

3.3. Normalized difference vegetation index (NDVI)

NDVI of the respective sampling sites were calculated from Landsat-7 (Fig. 5). NDVI suggest the normalization of scattering coefficient that will be the function of the vegetation characteristic of corresponding area. 69.56% of total sampling sites showed negative NDVI values, which denote that these areas (S1-S3, S6-S10, S12-S15, S17-S19 and S21-S23) are free from vegetation interference to radar signal ($\sigma°$) (Fig. 6). The rest

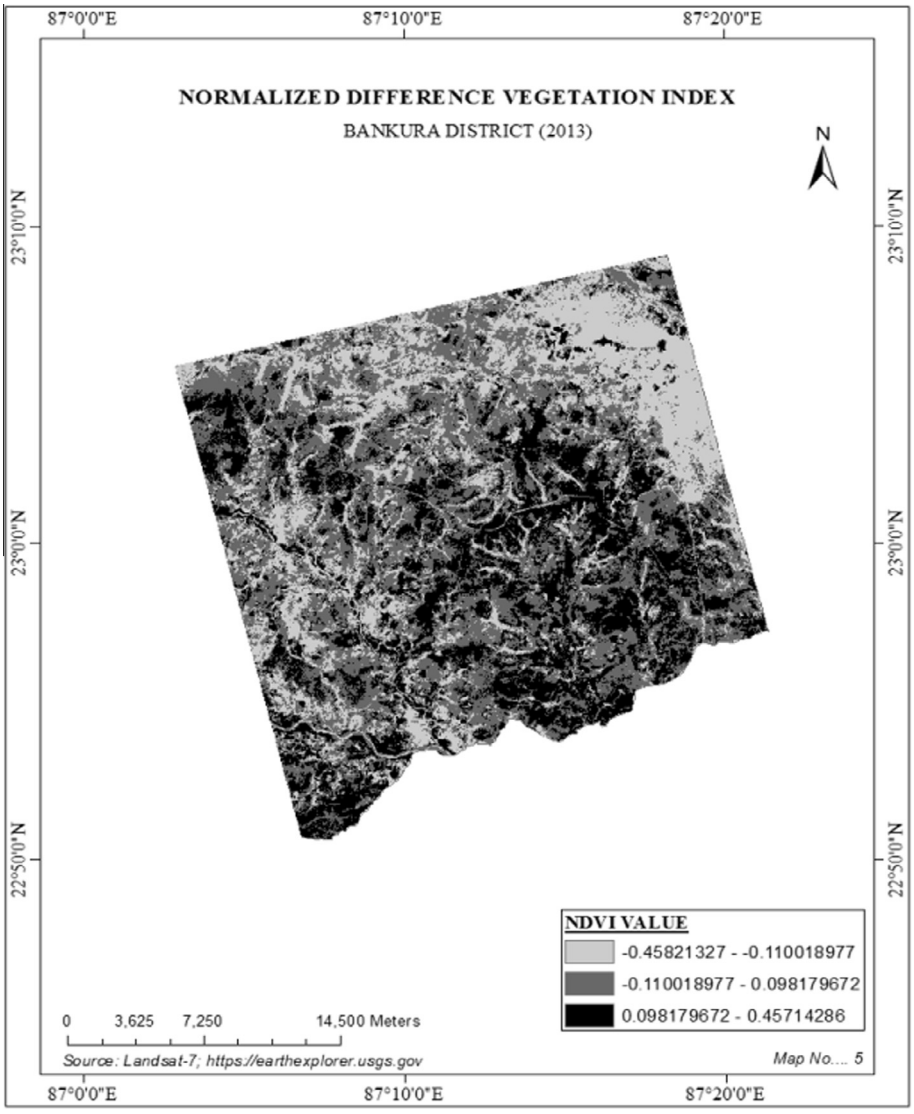

Figure 5 Normalize Difference Vegetation Index of Bankura district, covering part of Simlapal, Taldangra, Onda and Bishnupur block.

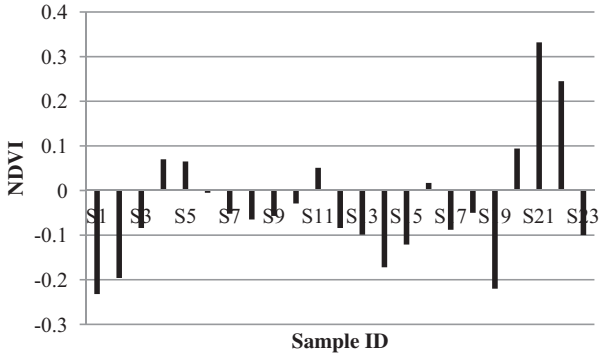

Figure 6 Sampling field wise NDVI value distribution.

of the 30.34% sampling sites which have smaller vegetation interferences are S4, S5, S11, S16 and S20-S22. Function of vegetation that gives an impact to σ°, this σ° can be correlated with NDVI, which represent the vegetation function only to σ°. So, there is a need to develop a relationship with NDVI for characterization of behavior of σ° (both RH and RV). The regression analysis shows that NDVI have a positive correlation with both the σ° (RH) and σ° (RV). Both have R^2 = 0.029 for σ° (RV) and R^2 = 0.001 for σ° (RH) (Fig. 7a and b). NDVI values of 23 respective sampling sites ranged from −0.232 to 0.332. The values of NDVI are within the range in which radar signal is not much affected (Dubois et al., 1995). Thus there was no need to minimize the effect of vegetation on radar backscattering signal.

3.4. Factors considered for soil moisture retrieval study

3.4.1. Backscattering coefficient (σ°)

Backscattering coefficient (σ°) of respective study area was calculated by using the Eq. (4). Image is processed to retrieve σ° (both RH and RV) by SARC-View. SARC-View is platform based application developed by NRSC particularly to process σ°. To process the image required value of calibration constant (K_{dB}), incidence angle for the pixel position p (i_p) and incidence angle at the scene center (c_{enter}) were taken from the metadata file. After that the image was processed and produced full resolution σ° in both RH and RV (Figs. 8 and 9). Derived σ° for RH and RV are represented in Figs. 8 and 9. σ° (RV) ranges from −21.360 to −5.640 dB with mean value −13.593 dB (±4.430). σ° for RH ranges from −23.950 to −7.150 dB with mean value −12.474 dB (±4.793) (Table 2):

$$\sigma^{\circ}(\mathrm{dB}) = 20\log_{10}(DN_p) - K_{\mathrm{dB}} + 10\log_{10}\left(\frac{Sin(i_p)}{Sin(i_{center})}\right) \quad (4)$$

3.4.2. Volumetric moisture content (M_v)

M_v for each of the 23 field samples was calculated by multiplying bulk density (*Sbd*) with gravimetric soil moisture (mg) value. Mean M_v for each of the 23 sites is 0.081 (±0.050) m^3/m^3 and ranges from 0.008 to 0.178 m^3/m^3. M_v for each of the sampling points is represented in Table 2.

3.4.3. Dielectric constant (ε)

Dielectric constants for each of the samples were calculated by using the Eq. (5) developed by Hallikainen et al., 1985. Where: s and c are the percentage of sand and clay by weight, and a_i, b_i, and c_i are the frequency dependent coefficients. ε is dielectric constant. ε ranged from 2.550 to 7.801 with an average of 4.410 (±1.578) (Table 2):

$$\varepsilon = (a_0 + a_1 s + a_2 c) + (b_0 + b_1 s + b_2 c) M_v + (c_0 + c_1 s + c_2 c) M_v^2 \quad (5)$$

3.4.4. Surface roughness (r.m.s.)

Surface roughness (*r.m.s.*) of that area is varying from 0.319 to 3.836 cm with an average value of 1.418 (±0.989) cm (Table 2). Surface roughnesses were measured to find out the sensitivity of *r.m.s.* on σ° (both RH and RV).

4. Analysis

4.1. Factors affecting SAR sensitivity to soil moisture

4.1.1. Relationship between backscattered radar signal and soil moisture

σ° versus M_v were plotted in the graph (Fig. 10a and b) for both polarization RH and RV. The results show that σ° to some extent depends on the M_v, which has a positive correlation. Results showed σ° increases with increasing M_v. σ° (RH) versus M_v and σ° (RV) versus M_v have R^2 = 0.588 and R^2 = 0.525 (Fig. 10a and b). Thus SAR backscatter is directly related to moisture content of the target under consideration. Fig. 10(a and b) illustrates the dynamics of the radar backscattering coefficient versus soil moisture for RH and RV polarization at high incidence angle (48.11°). Overall, the scattering behavior of the soil increased with soil moisture. The wide

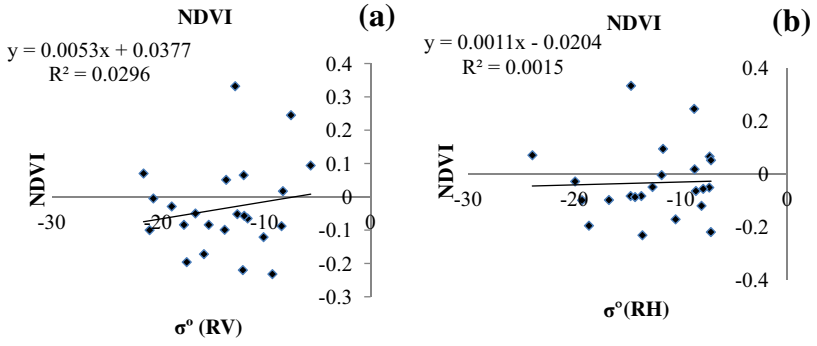

Figure 7 (a and b) Representation of simple linear regression between (a) σ° (RV) vs. NDVI and (b) σ° (RH) vs. NDVI.

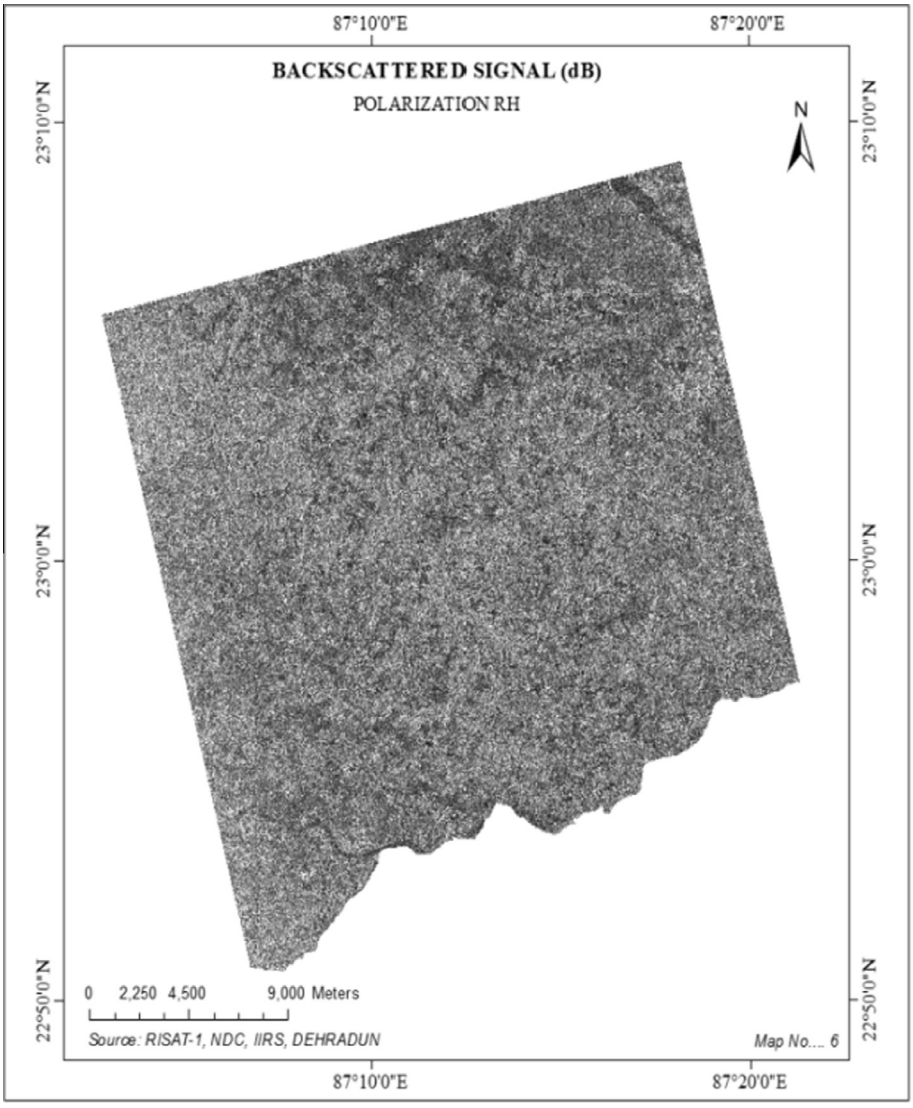

Figure 8 Backscattering coefficient (σ° RH) of processed image RISAT-1.

range of soil-moisture measurements made it possible to establish linear relationships between the radar signal and the soil moisture for each of the sampling sites.

4.1.2. Relationship between backscattered radar signal and di-electric constant

Dependency of σ° on dielectric property of soil is represented in Fig. 11(a and b). At microwave frequencies, dielectric constant of dry soil is around 3 and that of water is around 80 (Ulaby et al., 1982; Singh and Kathpalia, 2007). Hence dielectric constant for a moist soil, which is a mixture of the two, ranges between 2.550 and 7.801. When the dielectric constant of a material increases, it results in increase in σ° for both RH and RV (Dobson and Ulaby, 1981; Ulaby et al., 1986). Increasing trend of ε with σ° (RH) having $R^2 = 0.656$ (Fig. 11. a) and σ°(RV) having $R^2 = 0.534$ (Fig. 11. b). The dielectric behavior of the soil is also influenced by the distribution of the grain sizes and the amount of free water (Hallikainen et al., 1985; Mironov et al., 2004; Srivastava et al., 2006). Sandy soils have a higher amount of free water than clay soils which results in higher correlation between backscatter and soil moisture (Blumberg et al., 2000; Kong and Dorling, 2008; Srivastava et al., 2006; Walker et al., 2004).

4.1.3. Backscattered signal function of roughness

Random surface roughness was calculated in terms of route mean square surface height (*r.m.s.*) in each of the 23 sampling sites. σ° is highly sensitive to the *r.m.s.*, but in the present study *r.m.s.* did not show any significant relationship with the σ° for both polarizations (RH and RV). σ°(RH) with *r.m.s.* having $R^2 = 0.009$ (Fig. 12a) and σ°(RV) having $R^2 = 0.029$ (Fig. 12b). In spite of the fact that the images were taken at high incidence angles, where the influence of soil surface roughness is high, the roughness effect couldn't clearly be distinguished (Anguela et al., 2010). It might be because we have no roughness measurements on that date of satellite over passes. It may also be because the area is not corresponding to high *r.m.s.* values (0.319–3.836 cm). Different studies have demonstrated the agreement between real radar signals and theoretical surface backscattering models for the case of low

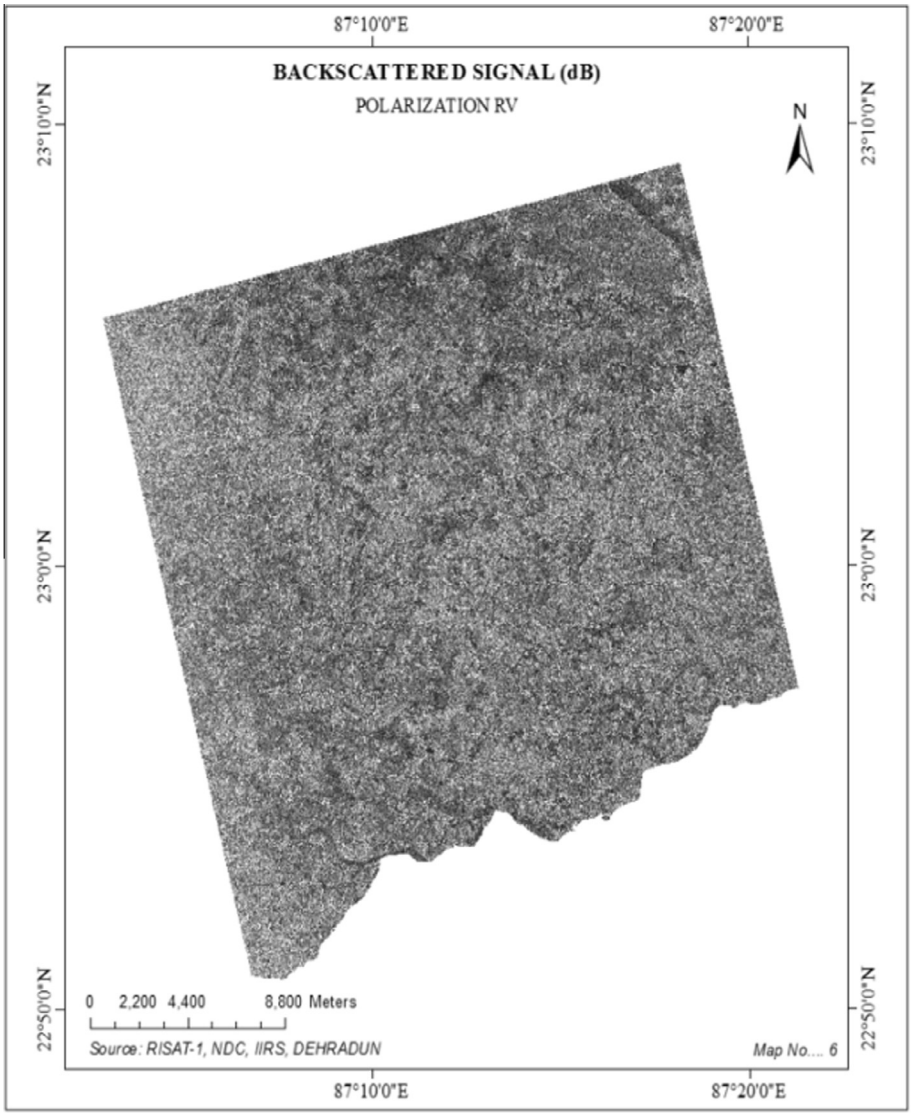

Figure 9 Backscattering coefficient (σ° RV) of processed image RISAT-1.

Table 2 Descriptive statistics of observed variables.

Variable	Minimum	Maximum	Mean	Std. deviation
M_v m^3/m^3	0.008	0.178	0.081	0.050
σ° (RV)	−21.360	−5.640	−13.593	4.430
σ° (RH)	−23.950	−7.150	−12.474	4.793
ε	2.544	7.801	4.410	1.578
r.m.s.	0.319	3.836	1.418	0.989

roughness and high moisture content (Chen et al., 1989; Anguela et al., 2010). Due to higher incidence angle in some of the cases the σ° has become independent on *r.m.s.* (Aubert et al., 2011).

4.1.4. Effects of soil texture on soil moisture

Difference in texture explains the difference in surface drying rate. For this reason, difficulties can be encountered in the interpretation of radar signals in cases where the vertical moisture profile varies strongly in the first centimeters (Anguela et al., 2010). In the C-band, decreasing soil clay content increases the sensitivity of the radar signal to soil moisture (Ulaby et al., 1978; Aubert et al., 2011). Because the distribution of grain sizes controls the amount of free water that interacts with the incident microwave, the amount of free water gives significant contribution to SAR backscatter (Srivastava et al., 2006, 2009; Aubert et al., 2011). To investigate these differences, soil samples were taken in each sampling site to determine the particle-size distribution within plots. According to the soil-composition analysis, the zones with low radar signal values (σ° RH: −7.28 dB and σ° RV: −11.94 dB) (darker zones) were more clayey (sample Id-S5: 49.08% clay, 30% silt and 20.92% sand) but an inverse result has been obtained for the Sample Id-S23 (Sample Id-S23: 47.08% clay, 22% silt and 30.92% sand) having higher radar signal value (σ° RH: −19.28 dB and σ° RV: −20.79 dB). Several studies in the C-band have shown that the radar signal is directly dependent on the amount of sand and clay, but only for soil compositions that are very difficult to explain and also the same hypothesis has been reflected from the results (Fig. 13) (Dobson and Ulaby, 1981; Schmugge et al., 1976; Ulaby et al., 1978).

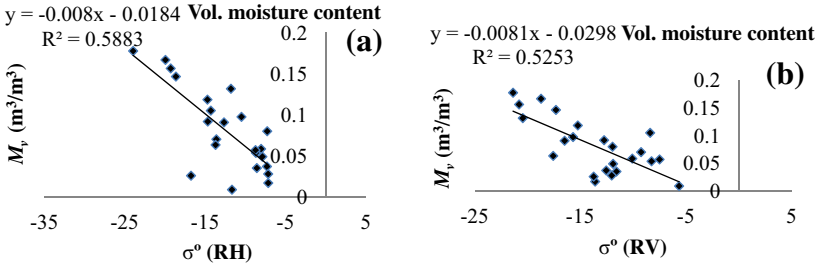

Figure 10 (a) Simple linear regression between σ° (RH) and M_v. (b) Simple linear regression between σ° (RV) and M_v.

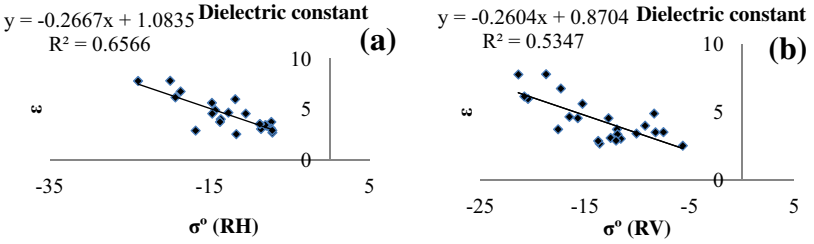

Figure 11 (a) Simple linear regression between σ° (RH) and ε. (b) Simple linear regression between σ° (RV) and ε.

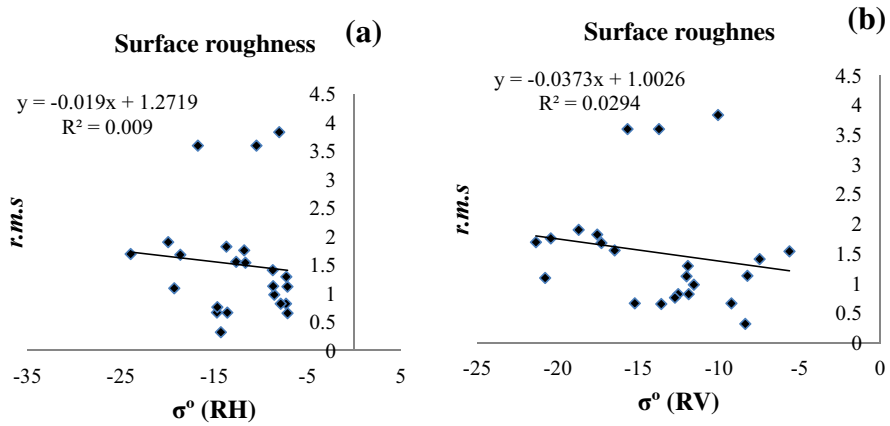

Figure 12 (a and b) Simple linear regression between (a) σ° (RH) and *r.m.s.* and (b) σ° (RV) and *r.m.s.*

4.2. Topp model

The Dielectric constant was derived from the Eq. (1). The soil moisture can be secondarily derived from the dielectric constant using (Topp et al., 1980) model. This model has been used by many researchers effectively for retrieving soil moisture (Song et al., 2010). This model derived soil moisture (θ_v) was used to validate with the ground truth soil moisture value. It has been found that θ_v versus M_v having $R^2 = 0.969$ (Fig. 14) shows good correspondence. As θ_v related with the ε, it has been proved that retrieved ε by using Eq. (1) of Hallikainen et al., 1985 is justified and true.

$$M_v = -5.3 \times 10^{-2} + 2.92 \times 10^{-2}\varepsilon - 5.5 \times 10^{-4}\varepsilon^2 + 4.3 \times 10^{-6}\varepsilon^3 \quad (6)$$

where: ε is di-electric constant and M_v is volumetric moisture content.

4.3. Semi-empirical model

Major influencing factors that affect the sensitivity of SAR sensor to retrieve volumetric soil moisture (M_v) were taken into consideration to derive a semi-empirical equation. To derive a semi-empirical model a multiple linear regression has been done, where M_v is considered as dependent variable and *r.m.s.*, ε, σ°(RH) and σ°(RV) considered as independent variables. Derived semi-empirical model is represented as Eq. (7). Validity of that model is statistically proved by the Goodness of fit (Table 3). This multiple linear regression model has adjusted $R^2 = 0.956$ and RMSE = 0.010 at 95% confidence level (Eq. (7)):

$$\mathrm{M_v\ (m^3/m^3)} = -5.63^{-02} - 1.91^{-04} * \sigma^{\circ}\ (\mathrm{RV}) + 8.84^{-04} * \sigma^{\circ}\ (\mathrm{RH}) + 3.27^{-02} * \varepsilon + 7.47^{-04} * \mathrm{RMS} \quad (7)$$

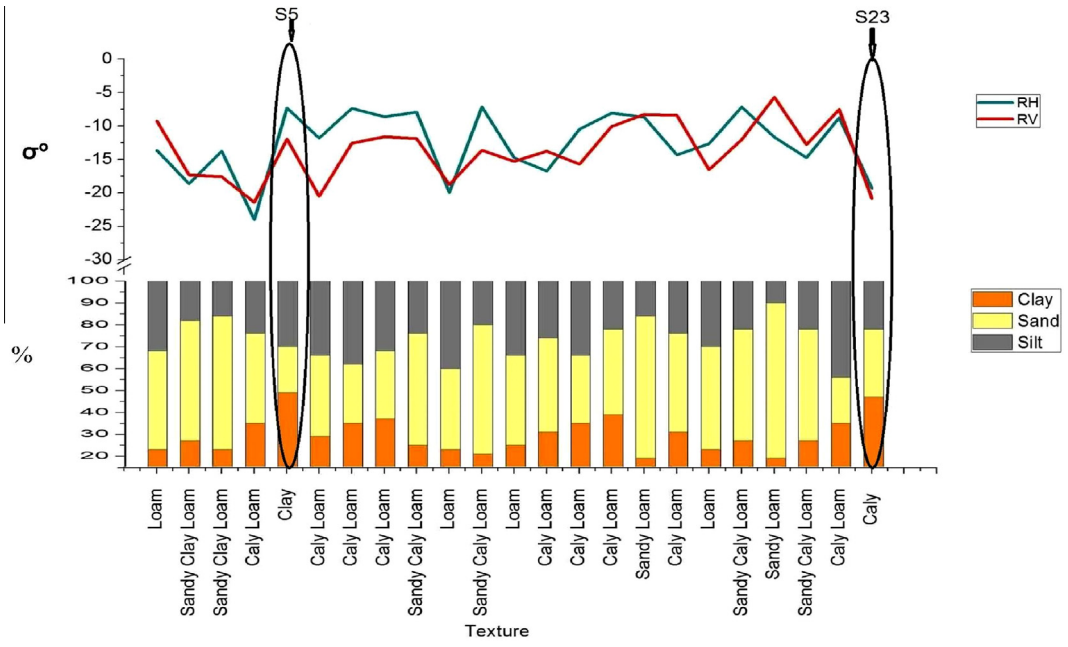

Figure 13 Behavior of backscattering coefficients (both $\sigma°$ RH and RV) for each sample soil textural configuration.

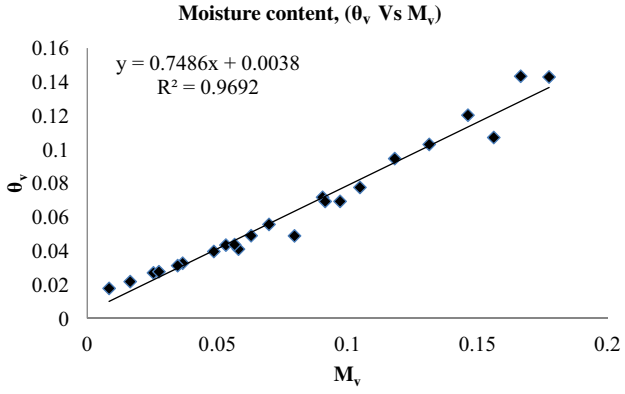

Figure 14 Relationship between estimated (M_v) and retrieved (Topp moisture content) soil volumetric moisture content.

Table 3 Regression of variable volumetric moisture m^3/m^3.

Goodness of fit statistics					
Observations	Sum of weights	R^2	Adjusted R^2	MSE	RMSE
23	23	0.964	0.956	0	0.01

5. Conclusion

Irrespective of field measurement a number of inversion models have been developed to retrieve soil moisture by using microwave remote sensing either active or passive. Synthetic Aperture Radar has shown its large potential for retrieving soil moisture maps at regional scales. However, since the backscattered signal is determined by several surface characteristics, the retrieval of soil moisture is an ill-posed problem when using single configuration imagery. The developed method here is more simple and realistic for the estimation of soil moisture. To develop this model major factors considered are $\sigma°$ (RH), $\sigma°$ (RV), ε and *r.m.s.* Derived $\sigma°$ for RH and RV ranges from -21.360 to -5.640 dB with mean value -13.593 dB (± 4.430). $\sigma°$ for RH ranges from -23.950 to -7.150 dB with mean value -12.474 dB (± 4.793). Mean M_v for each of the 23 sites is 0.081 (± 0.050) m^3/m^3 and ranges from 0.008 to 0.178 m^3/m^3. Derived ε ranges from 2.550 to 7.801 with an average of 4.410 (± 1.578). Surface roughness (*r.m.s.*) of that area is varying from 0.319 to 3.836 cm with an average value of 1.418 (± 0.989) cm. To compute this, model dependencies of each of the factors were considered and it was found as follows:

1. Backscattering coefficient ($\sigma°$) has a positive relationship with volumetric moisture content (M_v) both for $\sigma°$ (RH) and $\sigma°$ (RV) with $R^2 = 0.588$ and $R^2 = 0.525$.
2. The roughness component was derived in terms of root mean square height (*r.m.s.*) having a positive correlation with $\sigma°$ (RH) ($R^2 = 0.009$) and $\sigma°$ (RV) ($R^2 = 0.029$), but it was not so significant. The relationship between *r.m.s.* and $\sigma°$ (RH, RV) trend was justified enough to consider further in this study.
3. Dielectric constant (ε) has a positive relationship with $\sigma°$ (RH) having $R^2 = 0.656$ and $\sigma°$ (RV) having $R^2 = 0.534$.
4. According to the soil-composition analysis, the zones with low radar signal values ($\sigma°$ RH: -7.28 dB and $\sigma°$ RV: -11.94 dB) (darker zones) were more clayey (sample Id-S5: 49.08% clay, 30% silt and 20.92% sand) but an inverse result has been obtained for the Sample Id-S23 (Sample Id-S23: 47.08% clay, 22% silt and 30.92% sand) having higher radar signal value ($\sigma°$ RH: -19.28 dB and $\sigma°$ RV: -20.79 dB).
5. Topp model derived soil moisture (θ_v) was used to validate with the ground truth soil moisture value. It has been found that θ_v versus M_v having $R^2 = 0.968$. As θ_v related with the

ε, it has been proved that retrieved ε by using Eq. (1) of Hallikainen et al., 1985 is justified and true. Considering all the major influencing factors (σ° (RH), σ° (RV), ε and *r.m.s.*) for soil moisture retrieval (M_v) a semi-empirical model has been developed (Eq. (7)), where M_v is a function of σ° (RH), σ° (RV), ε and *r.m.s.* This model has adjusted $R^2 = 0.956$ and RMSE = 0.010 at 95% confidence level. On the basis of input data considering all the factors, statistical retrieval of soil moisture against predicted value has been justified. This predicted value is derived from this linear regression model. This model has an $R^2 = 0.963$ of observed versus predicted soil moisture value.

Acknowledgement

WorldView-2 satellite sensor image was provided by the Fishery Mapping Project, Awareness Centre, Sector IV, Salt Lake, Kolkata. Also thanks to Dr. Sisir Kumar Si, Soil Scientist and Incharge Soil, Water and Manure Testing Laboratory Vivekananda Institute of Biotechnology Sri R. K. Ashram, Nimpith, South 24 Pgs, W. B., for his kind suggestion and help to analyze soil parameters.

References

Álvarez-Mozos, J., Casali, J., Gonzalez-Audicana, M., Verhoest, N. E.C., 2005. Correlation between ground measured soil moisture and RADARSAT-1 derived backscattering coefficient over an agricultural catchment of Navarre (north of Spain). Biosyst. Eng. 92 (1), 119–133. http://dx.doi.org/10.1016/j.biosystemseng.2005.06.008.

Al-Yaari, A., Wigneron, J.P., Ducharne, A., Kerr, Y.H., Wagner, W., De Lannoy, G., Reichle, R., Al Bitar, A., Dorigo, W., Richaume, P., Mialon, A., 2014. Global-scale comparison of passive (SMOS) and active (ASCAT) satellite based microwave soil moisture retrievals with soil moisture simulations (MERRA-Land). Remote Sens. Environ. 152, 614–626.

Anguela, T.P., Zribi, M., Baghdadi, N., Loumagne, C., 2010. Analysis of local variation of soil surface parameters with TerraSAR-X radar data over bare agricultural fields. IEEE Trans. Geosci. Remote Sens. 48 (2), 874–881.

Aubert, M., Baghdadi, N., Zribi, M., Douaoui, A., Loumagne, C., Baup, F., El Hajj, M., Garrigues, S., 2011. Analysis of TerraSAR-X data sensitivity to bare soil moisture, roughness, composition and soil crust. Remote Sens. Environ. 115, 1801–1810.

Baghdadi, N., Aubert, M., Cerdan, O., Franchisteguy, L., Viel, C., Martin, E., Zribi, M., Desprats, J.F., 2007. Operational mapping of soil moisture using synthetic aperture radar data: application to the Touch basin (France). Sensors 7, 2458–2483.

Baghdadi, N., Zribi, M., 2006. Evaluation of radar backscatter models IEM, OH and Dubois using experimental observations. Int. J. Remote Sens. 27 (18), 3831–3852. http://dx.doi.org/10.1080/01431160600658123.

Baghdadi, N., King, C., Chanzy, A., Wigneron, J.P., 2002a. An empirical calibration of the integral equation model based on SAR data, soil moisture and surface roughness measurement over bare soils. Int. J. Remote Sens. 23 (20), 4325–4340. http://dx.doi.org/10.1080/01431160110107671.

Baghdadi, N., King, C., Bonnifait, L., 2002b. An empirical calibration of the Integral equation model based on SAR data and soil parameters measurements. Geoscience and Remote Sensing Symposium, IGARSS '02. 2002 IEEE International, 2646–2650. doi: http://dx.doi.org/10.1109/IGARSS.2002.1026729.

Baghdadi, N., Holah, N., Zribi, M., 2006. Soil moisture estimation using multi-incidence and multi-polarization ASAR data. Int. J. Remote Sens. 27 (10), 1907–1920. http://dx.doi.org/10.1080/01431160500239032.

Baghdadi, N., Cerdan, O., Zribi, M., Auzet, V., Darboux, F., El Hajj, M., Bou Kheir, R., 2008. Operational performance of current synthetic aperture radar sensors in mapping soil surface characteristics in agricultural environments: application to hydrological and erosion modeling. Hydrol. Process. 22 (1), 9–20. http://dx.doi.org/10.1002/hyp.6609.

Baghdadi, N., Aubert, M., Zribi, M., 2012. Use of TerraSAR-X data to retrieve soil moisture over bare soil agricultural fields. IEEE Geosci. Remote Sens. Lett. 9 (3), 512–516.

Batlivala, P.P., Ulaby, F.T., 1977. Feasibility of monitoring soil moisture using active microwave remote sensing Remote Sensing Laboratory. Tech. Rep., 264–12, University of Kansas, Lawrence.

Bertoldi, G., Chiesa, S.D., Notarnicola, C., Pasolli, L., Niedrist, G., Tappeiner, U., 2014. Estimation of soil moisture patterns in mountain grasslands by means of SAR RADARSAT2 images and hydrological modeling. J. Hydrol. 516, 245–257.

Blumberg, D.G., Freilikher, V., Lyalko, I.V., Vulfson, L.D., Kotlyar, A.L., Shevchenko, V.N., Ryabokonenko, A.D., 2000. Soil moisture (water-content) assessment by an airborne scatterometer: the Chernobyl disaster area and the Negev desert. Remote Sens. Environ. 71 (3), 309–319. http://dx.doi.org/10.1016/S0034-4257(99)00087-5.

Chen, J.M., Yang, B.J., Zhang, R.H., 1989. Soil thermal emissivity as affected by its water content and surface treatment. Soil Sci. 148, 433.

Dobson, M.C., Ulaby, F.T., 1981. Microwave backscatter dependence on surface roughness, soil moisture, and soil texture: Part III-soil tension. IEEE Trans. Geosci. Remote Sens. 19 (1), 51–61. http://dx.doi.org/10.1109/TGRS.1981.350328.

Dobson, M.C., Ulaby, F.T., 1986. Active microwave soil moisture research. IEEE Trans. Geosci. Remote Sens. 24 (1), 23–36. http://dx.doi.org/10.1109/TGRS.1986.289585.

Dubois, P., Van Zyl, J., Engman, T., 1995. Measuring soil moisture with imaging radars. IEEE Trans. Geosci. Remote Sens. 33 (4), 915–926. http://dx.doi.org/10.1109/36.406677.

Engman, E.T., 1990. Progress in microwave remote sensing of soil moisture. Can. J. Remote Sens. 16 (3), 6–14.

Engman, E.T., 1991. Applications of microwave remote sensing of soil moisture for water resources and agriculture. Remote Sens. Environ. 35 (2–3), 213–226. http://dx.doi.org/10.1016/0034-4257(91)90013-V.

Fung, A.K., 1994. Microwave Scattering and Emission Models and their Applications. Artech House, Nordwood, USA.

Fung, A.K., Chen, K.S., 1992. Dependence of the surface backscattering coefficients on roughness, frequency and polarization states. Int. J. Remote Sens. 13 (9), 1663–1680. http://dx.doi.org/10.1080/01431169208904219.

Gharechelou, S., Tateishi, R., Tetuko, J., Sumantyo, S., 2015. Interrelationship analysis of L-band backscattering intensity and soil dielectric constant for soil moisture retrieval using PALSAR data. Adv. Remote Sens. 4, 15–24.

Hallikainen, M.T., Ulaby, F.T., Dobson, M.C., Elrayes, M.A., Wu, L. K., 1985. Microwave dielectric behavior of wet soil. 1: empirical models and experimental observations. IEEE Trans. Geosci. Remote Sens. 23 (1), 25–34. http://dx.doi.org/10.1109/TGRS.1985.289497.

Holah, N., Baghdadi, N., Zribi, M., Bruand, A., King, C., 2005. Potential of ASAR/ENVISAT for the characterization of soil surface parameters over bare agricultural fields. Remote Sens. Environ. 96 (1), 78–86. http://dx.doi.org/10.1016/j.rse.2005.01.008.

Kong, X., Dorling, S.R., 2008. Near-surface soil moisture retrieval from ASAR wide swath imagery using a principal component analysis. Int. J. Remote Sens. 29 (10), 2925–2942. http://dx.doi.org/10.1080/01431160701442088.

Kornelsen, K.C., Coulibaly, P., 2013. Advances in soil moisture retrieval from synthetic aperture radar and hydrological applications. J. Hydrol. 476 (2013), 460–489.

Laguardia, G., Niemeyer, S., 2008. On the comparison between the LISFLOOD modelled and the ERS/SCAT derived soil moisture estimates. Hydrol. Earth Syst. Sci. 12, 1339–1351.

Le Hégarat Mascle, S., Zribi, M., Alem, F., Weisse, A., Loumagne, C., 2002. Soil moisture estimation from ERS/SAR data: toward an operational methodology. IEEE Trans. Geosci. Remote Sens. 40 (12), 2647–2658.

Li, Y.Y., Zhao, K., Ren, J.H., Ding, Y.L., Wu, L.L., 2014. Analysis of the dielectric constant of saline-alkali soils and the effect on radar backscattering coefficient: a case study of soda alkaline saline soils in western Jilin Province using RADARSAT-2 data. Sci. World J., 1–14 http://dx.doi.org/10.1155/2014/56301.

Mironov, V.L., Dobson, M.C., Kaupp, V.H., Komarov, S.A., Kleshchenko, V.N., 2004. Generalized refractive mixing dielectric model for moist soils. IEEE Trans. Geosci. Remote Sens. 42 (4), 773–785.

Oh, Y., 2004. Quantitative retrieval of soil moisture content and surface roughness from multipolarized radar observations of bare soil surfaces. IEEE Trans. Geosci. Remote Sens. 42 (3), 596–601. http://dx.doi.org/10.1109/TGRS.2003.821065.

Petropoulos, G.P., Ireland, G., Barrett, B., 2015. Surface soil moisture retrievals from remote sensing: Current status, products and future trends. Phys. Chem. Earth (in press).

Saleh, A., 1993. Soil roughness measurement: chain method. J. Soil Water Conserv. 48CG, 527–529.

Schmugge, T., Wilheit, T., Webster, W., Gloerson, P., 1976. Remote sensing of soilmoisture with microwave radiometers-II. NASA Technical Note TN-D-8321. Greenbelt, MD, 20771, NASA Goddard Space Flight Center.

Seneviratne, S.I., Corti, T., Davin, E.L., Hirschi, M., Jaeger, E.B., Lehner, I., Orlowski, B., Teuling, A.J., 2010. Investigating soil moisture-climate interactions in a changing climate: a review. Earth Sci. Rev. 99 (3-4), 125–161.

Shi, J., Wang, J., Hsu, A.Y., O'Neill, P.E., Engman, E.T., 1997. Estimation of bare surface soil moisture and surface roughness parameter using L band SAR image data. IEEE Trans. Geosci. Remote Sens. 35 (5), 1254–1266.

Singh, D., Kathpalia, A., 2007. An efficient modeling with ga approach to retrieve soil texture, moisture and roughness from Ers-2 SAR data. Prog. Electromagnet. Res. 77, 121–136. http://dx.doi.org/10.2528/PIER07071803.

Song, K., Zhou, X., Fan, Y., 2010. Retrieval of soil moisture content from microwave backscattering using a modified IEM model. Prog. Electromagnet. Res. B 26, 383–399. http://dx.doi.org/10.2528/PIERB10072905.

Srivastava, H.S., Patel, P., Manchanda, M.L., Adiga, S., 2003. Use of multiincidence angle RADARSAT-1 SAR data to incorporate the effect of surface roughness in soil moisture estimation. IEEE Trans. Geosci. Remote Sens. 41 (7), 1638–1640. http://dx.doi.org/10.1109/TGRS.2003.813356.

Srivastava, H.S., Patel, P., Navalgund, R.R., 2006. How far SAR has fulfilled its expectation for soil moisture retrieval? Microwave Remote Sensing of Atmosphere and Environment-II, AE107, Asia Pacific Remote Sensing Symposium, 13–17 November, 2006, Goa, India. SPIE Digital Library, 6410, Paper No. 64100, pp. 1–12.

Srivastava, H.S., Patel, P., Sharma, Y., Navalgund, R.R., 2009. Large-area soil moisture estimation using multi-incidence-angle RADARSAT-1 SAR data. IEEE Trans. Geosci. Remote Sens. 47 (8), 2528–2534. http://dx.doi.org/10.1109/TGRS.2009.2018448.

Topp, G.C., Davis, J.L., Annan, A.P., 1980. Electromagnetic determination of soil water content: measurements in coaxial transmission lines. Water Resour. Res. 16 (3), 574–582. http://dx.doi.org/10.1029/WR016i003p00574.

Ulaby, F.T., Batlivala, P.P., Dobson, M.C., 1978. Microwave backscatter dependence on surface roughness, soil moisture, and soil texture: Part I-Bare soil. IEEE Trans. Geosci. Remote Sens. GE-16 (4), 286–295.

Ulaby, F., Moore, R.K., Fung, A.K., 1982. Microwave Remote Sensing-Active and Passive. Addison Wesley, 2-3.

Ulaby, F.T., Moore, R.K., Fung, A.K., 1986. In: Microwave Remote Sensing: Active and Passive, vol. 3. Addison-Wesley Publishers, Reading, Mass.

Wagner, W., Blöschl, G., Pampaloni, P., Calvet, J.-C., Bizzarri, B., Wigneron, J.-P., Kerr, Y., 2007. Operational readiness of microwave remote sensing of soil moisture for hydrologic applications. Nord. Hydrol. 38 (1), 1–20. http://dx.doi.org/10.2166/nh.2007.029.

Walker, J.P., Houser, P.R., Willgoose, G.R., 2004. Active microwave remote sensing for soil moisture measurement: a field evaluation using ERS-2. Hydrol. Processes 18 (11), 1975–1997.

Wood, E.F., Lettenmaier, D.P., Zartarian, V.G., 1992. A landsurface hydrology parameterization with subgrid variability for general circulation models. J. Geophys. Res. 97, 2717–2728.

Zhao, W., Li, Z.L., 2013. Sensitivity study of soil moisture on the temporal evolution of surface temperature over bare surfaces. Int. J. Remote Sens. 34 (9–10), 3314–3331.

Zribi, M., Dechambre, M., 2002a. A new empirical model to retrieve soil moisture and roughness from C-band radar data. Remote Sens. Environ. 84, 42–52.

Zribi, M., Dechambre, M., 2002b. A new empirical model to retrieve soil moisture and roughness from C-band radar data. Remote Sens. Environ. 84 (1), 42–52. http://dx.doi.org/10.1016/S0034-4257(02)00069-X.

Zribi, M., Baghdadi, N., Holah, N., Fafin, O., 2005. New methodology for soil surface moisture estimation and its application to ENVISAT-ASAR multi-incidence data inversion. Remote Sens. Environ. 96, 485–496.